

# Evolution of boron-interstitial clusters in crystalline Si studied by transmission electron microscopy

S. Boninelli,<sup>a)</sup> S. Mirabella,<sup>b)</sup> E. Bruno, and F. Priolo

MATIS CNR-INFM and Dipartimento di Fisica ed Astronomia, Università di Catania,  
Via Santa Sofia 64, 95123 Catania, Italy

F. Cristiano

LAAS-CNRS, 7 Avenue du Colonel Roche, 31077 Toulouse, France

A. Claverie

CEMES-CNRS, 29 Rue Jeanne Marvig, 31055 Toulouse, France

D. De Salvador, G. Bisognin, and E. Napolitani

MATIS CNR-INFM and Dipartimento Fisica, Università di Padova, Via F. Marzolo 8, 35131 Padova, Italy

(Received 27 March 2007; accepted 19 June 2007; published online 16 July 2007)

The thermal evolution of large boron-interstitials clusters (BICs) in crystalline Si has been studied by transmission electron microscopy (TEM). After ion implantation (20 keV and  $1 \times 10^{14}$  Si/cm<sup>2</sup>) and annealing (815 °C and 5 min), large clusters (6–8 nm) have been observed in correspondence of a narrow, highly doped Si:B layer ( $2 \times 10^{20}$  B/cm<sup>3</sup>). Under prolonged annealing, such clusters dissolve, progressively shrinking their mean size below the TEM detection limit. The time evolution of such a BIC shrinking is fully compatible with the slow path dissolution kinetics recently published. These data suggest the identification of the slow dissolving BICs with the large observed clusters. © 2007 American Institute of Physics. [DOI: 10.1063/1.2757145]

The continuous miniaturization of complementary metal-oxide-semiconductor devices in microelectronics demands the fabrication of ultrashallow and highly doped *p/n* junctions in crystalline Si (*c*-Si). In order to obtain increasing B doping, this element is implanted in Si at fluences so high to overcome its solid solubility limit in *c*-Si. As a consequence of such a high B concentration and of the crystal damage caused by implantation, during the following annealing, B and self-interstitials (Is) precipitate in clusters, called boron-interstitial clusters (BICs).<sup>1–7</sup> These BICs are detrimental for electrical applications as a result of both B deactivation and crystal defect agglomeration.

Despite their crucial importance, little is known of BICs. From *ab initio* calculations, it is expected that BICs contain only few atoms.<sup>2,8</sup> For this reason, little efforts have been put to detect and identify them by transmission electron microscopy (TEM). Nonetheless, Cristiano *et al.*<sup>9</sup> observed by weak beam dark field (WBDF) analyses, quite large BICs, containing hundred of atoms, produced by low energy (500 eV) and high fluence ( $1 \times 10^{15}$  B/cm<sup>2</sup>) B implantation in Si. They further observed, by using high resolution electron microscopy, that these BICs appear as small extrinsic dislocation loops lying on {100} planes, i.e., two-dimensional precipitates. Five crystallographic variants, characterized by different Burgers vectors, have been identified.<sup>10</sup> For this reason, the visibility and apparent density of BICs dramatically depend on the conditions used for imaging. It was then shown that during annealing these BICs undergo an Ostwald ripening phenomenon.

Recently, it has been demonstrated that BIC dissolution under annealing occurs through two different paths with two

distinct dissolution times (fast and slow dissolving BICs).<sup>7</sup> A direct evidence of this hypothesis was not supplied since neither microscopic investigation on these two well defined BIC families nor on their respective size was performed. Moreover, if BIC dissolution has been well characterized by means of secondary ion mass spectrometry (SIMS) profile analyses, no detailed microscopy study has been conducted on the dissolution of such precipitates.

In this letter, we report a TEM study of the thermal evolution of B clusters formed by Si implantation of Si samples containing a buried, highly doped Si:B layer. We will show that a considerable fraction of these clusters are visible by TEM and that they are connected to the slow dissolving fraction of the cluster population. TEM images show that their dimension gradually reduces under annealing up to their complete disappearance.

The samples were prepared by molecular beam epitaxy (MBE) on a 5 in.,  $2 \times 1$  reconstructed (100) Si substrate, as described in Ref. 7. The samples, with a B box of  $2 \times 10^{20}$  B/cm<sup>3</sup> at the depth of 220 nm, were then implanted with 20 keV Si ions (projected range of about 30 nm) with a nonamorphizing dose of  $1 \times 10^{14}$  ions/cm<sup>2</sup> (see drawing of Fig. 1). The substitutionality of the starting B box was verified, as reported in Ref. 7. A rapid thermal annealing at 815 °C for 5 min was performed to fully dissolve the implant induced defects and inject Is toward the B box.<sup>11</sup> Such Is interact with B causing the formation of BICs. Hereinafter we will refer to this sample as the “as formed” one. This sample was cut into small pieces, that were subjected to various thermal treatments at 815 and 1000 °C, for times ranging between 10 s and 16 h. A 200 keV JEOL 2010-HC TEM was used for the structural study. Analyses in cross-sectional view were performed in WBDF, with  $g=400$  (where  $g$  is the diffracting vector used to take the images), in order to reveal the presence of BICs. The atomic concentration of B was

<sup>a)</sup>Electronic mail: simona.boninelli@ct.infn.it

<sup>b)</sup>Author to whom correspondence should be addressed; electronic mail: mirabella@ct.infn.it

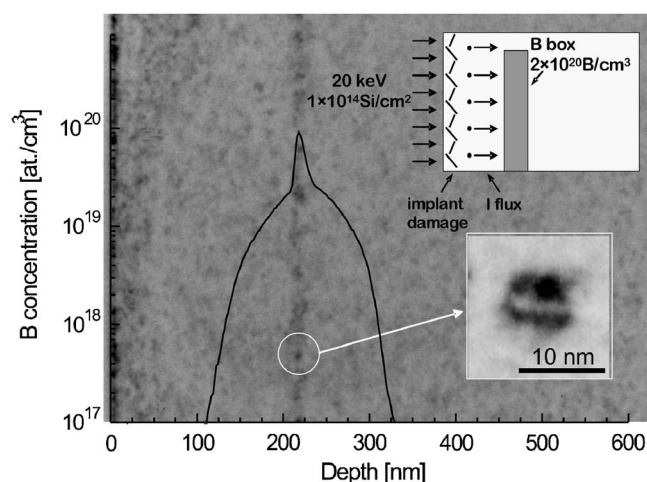


FIG. 1. SIMS boron profile overlapped with WBDF TEM cross-sectional view (negative images) of the as formed sample. In the inset, a higher magnified image of a BIC. A schematic of the experiment is also shown.

determined by SIMS, using a CAMECA IMS-4f instrument, with a 3 keV  $O_2^+$  analyzing beam. It should be emphasized that our experimental conditions were accurately chosen in order to spatially separate the implantation related damage from the B box<sup>5-7</sup> allowing us to accurately monitor the I flux from the damaged area towards the B box during the annealing. Thus, we had the chance to study the microscopic mechanisms of BIC formation and dissolution more accurately than what occurs in B implanted samples where the implanted damaged region overlaps the doped region.

In Fig. 1, a WBDF cross-sectional view (negative image) of the as formed sample is reported, showing a band of clusters, at about 220 nm below the surface, appearing as dark spots (3–4 nm in radius) on a grey background. It is interesting to note the total absence of extended defects at about 30 nm below the surface, indicating that they have been fully dissolved after the thermal annealing.

SIMS B profile, obtained from the same sample, is superimposed on the same figure. It presents the usual features of such experimental conditions, i.e., a static peak, whose kink is at about  $2.3 \times 10^{19}$  B/cm<sup>3</sup>, and a fast-diffusing tail. The static peak indicates the presence of the nondiffusing B just in correspondence with the clusters showed by the TEM image, clearly demonstrating that these precipitates must contain B atoms. Moreover, from higher magnification images (as shown in the inset) it has been observed that these defects display the typical contrast of dislocation loops. This suggests, in agreement with Refs. 9 and 10, that these defects have a two-dimensional shape and consist also of Si interstitials. It is therefore possible to conclude that these clusters, being formed by both B atoms and Is, are large BICs.

The dose of clustered B in the as formed sample is equal to  $6.5 \times 10^{13}$  B/cm<sup>2</sup> (Ref. 7) while, by simulation of B diffusion and by comparison with a sample with no B box with the same method described in Refs. 5 and 8, the dose of Is involved in BIC formation is estimated to be about  $1.5 \times 10^{13}$  Si/cm<sup>2</sup>. Based on these data, we can state that the average composition of these BICs results to be shifted toward B rich precipitates (B:Si ratio of  $\sim 4$ ), as suggested by theoretical calculations.<sup>12,13</sup> This high quantity of B over Si atoms suggests that B atoms strongly influence the lattice deformation around each BIC as confirmed by strain measurements.<sup>14</sup>

To obtain a reliable estimation of the BIC density, plan view analyses should be realized, but in our case BICs are extremely small precipitates, placed too far below the surface. This implies that in plan view configuration the BIC contrast, especially for the smallest ones, is attenuated by the overhanging 220-nm-thick Si layer and, as a consequence, their signal is hardly distinguishable from the background. On the other hand, this problem is not present in cross-sectional analyses, which furnish a satisfactory estimation of the BIC mean sizes. To roughly evaluate the areal density  $\sigma_{\text{BICs}}$  of BICs visible by TEM, we proceeded as follows. We assumed the following formula:

$$\sigma_{\text{BICs}} = \frac{N}{\rho A}, \quad (1)$$

where  $N \sim 8 \times 10^{13}$  at./cm<sup>2</sup> is the dose of atoms precipitated in BICs (both B and Si),<sup>7</sup>  $A$  is the mean area of a BIC (about  $\sim 4 \times 10^{-13}$  cm<sup>2</sup>) obtained by the mean radius value measured by TEM and by assuming a circular shape (as for dislocation loops) for all the clusters, while  $\rho$  is the atomic density of BICs per unit area. Since this last value is unknown, we have assumed that  $\rho$  is equal to the atomic density per unit area of the {100} family planes in Si ( $13.5 \times 10^{14}$  Si/cm<sup>2</sup>).<sup>9</sup> The result of such an exercise is  $\sigma_{\text{BICs}} \sim 1.5 \times 10^{11}$  BICs/cm<sup>2</sup>, about an order of magnitude lower than that reported in Ref. 9. This is probably due to the lower B concentration present in our samples. It is worth noting that such a value of density is underestimated since a certain amount of  $N$  is presumably stored in smaller BICs, whose size is below the TEM detection limit.

Recently, we showed that such as formed BICs belong to two families undergoing different paths in the dissolution process (slow and fast path). In particular, in this sample about 80% of the as formed BICs follow a slow dissolving path.<sup>7</sup> Therefore, at this stage we can argue that this observed BICs are those connected to the slow dissolution.

Once BICs have been formed, we investigated their thermal evolution by varying both the annealing temperature and the annealing time. Cross-sectional TEM images of these samples are shown in Fig. 2. In particular, the as formed samples further annealed at 815 °C for 105 min and for 16 h are reported in Figs. 2(a) and 2(b), respectively. The BIC band is still visible, although a confident evaluation of their mean size is a very difficult task, owing to their extremely small dimension (less than 3 nm in radius). Nevertheless, we can qualitatively state that after further annealing BICs tend to shrink. It is worth noting that all BICs present in both these samples belong to the slow dissolving family, since the fast dissolution phase has been definitely extinguished.<sup>7</sup>

A quite similar scenario is shown by the TEM images of the as formed samples further annealed at 1000 °C for 10 s [Fig. 2(c)] and 60 s [Fig. 2(d)]. Indeed, also after 10 s the defect band shows very small clusters (less than 3 nm) while after 60 s no defects are detected at all. Also in this case, all the BICs belong to the slow dissolving family.<sup>7</sup> These evidences support the hypothesis that BICs observed by TEM ever belong to the slow dissolving family and that fast dissolving BICs are smaller and undetectable by TEM, as suggested in Ref. 7. Figure 2(d) tells us that after 1000 °C for 60 s, BICs are completely dissolved or their size is below the TEM detection limit (i.e., below 1–2 nm).

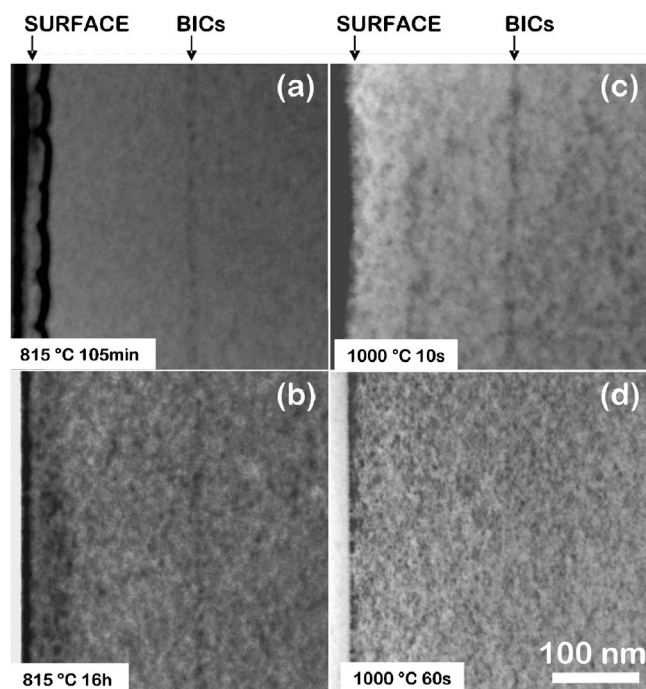


FIG. 2. WBD F TEM cross-sectional view (negative images) of the as formed sample further annealed at 815 °C for (a) 105 min or (b) 16 h, and at 1000 °C for (c) 10 s or (d) 60 s.

To exploit this point we report in Fig. 3 the SIMS profiles of both the samples annealed at 815 °C for 16 h (open squares) and 1000 °C for 60 s (closed squares). It is clear that BICs persist for both samples, as evidenced by the immobile peaks in Fig. 3. In the 815 °C, 16 h sample the B clustered dose is equal to  $4.2 \times 10^{13}$  B/cm<sup>2</sup>, while in the 1000 °C, 60 s sample it is equal to  $2.5 \times 10^{13}$  B/cm<sup>2</sup>. Thus, even if BICs are still present after 1000 °C for 60 s, their size is presumably too small to be detectable by TEM.

This implies that (i) a sort of dose threshold exists for clustered B to make BICs visible by TEM and (ii) the

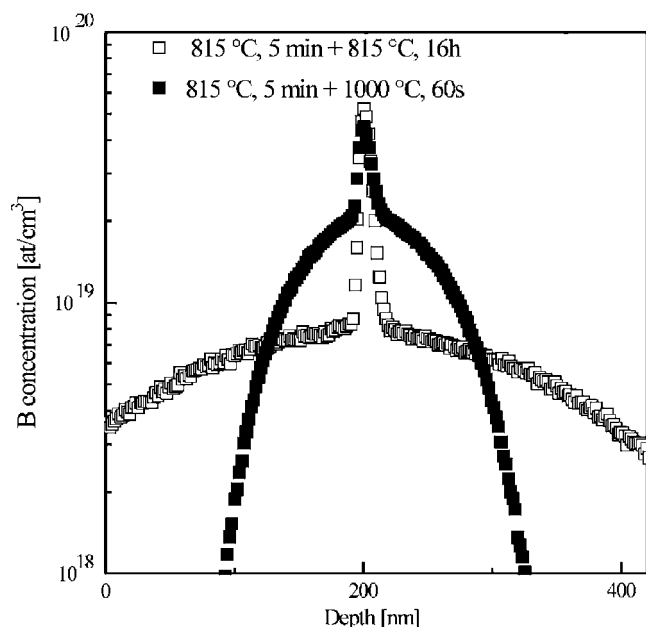


FIG. 3. SIMS boron profile of the as formed sample further annealed at 815 °C for 16 h (open squares) and at 1000 °C for 60 s (closed squares).

1000 °C annealing results to be more effective in reducing B cluster dimensions. On the other hand, Fig. 3 tells us that the B diffusion is greater at the lower temperature. This agrees with the different activation energies for slow-path BIC dissolution (4.8 eV) and B diffusion (3.1–3.8 eV).<sup>7,15</sup>

Finally, a last comment should be made. Our results showed a gradual shrinkage of BICs during prolonged annealing. This mechanism seems in contrast with the Ostwald ripening mechanism proposed by Cristiano *et al.*<sup>9</sup> Actually, in that case the higher B concentration ( $\sim$  a factor of 10) and the location of B within the implanted damaged region should lead to quite different precipitates, presumably larger and richer in Is with respect to our case. In addition, in that paper the thermal dissolution regime has not been exploited. Thus, one can assume that during early stages of annealing an Ostwald ripening occurs, provided that a high enough BIC density leads to a BIC growth. Later on, when BIC density is reduced, BICs stop to grow and start to dissolve.

In conclusion, we observed by TEM very large BICs, formed in correspondence with the B box, with a dislocation loop shape. Such BICs belong to the slow dissolving family, which presumably is characterized by larger clusters. Once BICs have been formed, during prolonged thermal annealing their mean size progressively reduces till it falls below the TEM detection limit. Thus, in addition to an Ostwald ripening mechanism, a subsequent phase occurs during which BIC density is quite low and their mean size shrinks, with the shrinking being more effective at higher temperatures.

The authors wish to thank M. G. Grimaldi, G. Impellizzeri, and C. Percolla (CNR-INFM MATIS), A. Marino (CNR-IMM), and R. Storti (University of Padova) for their assistance.

<sup>1</sup>W. K. Hofker, H. W. Werner, D. P. Oosthoek, and H. A. M. de-Grefte, *Appl. Phys.* **2**, 165 (1973).

<sup>2</sup>S. Solmi, F. Baruffaldi, and R. Canteri, *J. Appl. Phys.* **69**, 2135 (1991).

<sup>3</sup>N. E. B. Cowern, K. T. F. Janssen, and H. F. F. Jos, *J. Appl. Phys.* **68**, 6191 (1990).

<sup>4</sup>L. Pelaz, M. Jaraiz, G. H. Gilmer, H.-J. Gossmann, C. S. Rafferty, D. J. Eaglesham, and J. M. Poate, *Appl. Phys. Lett.* **70**, 17 (1997).

<sup>5</sup>S. Mirabella, E. Bruno, F. Priolo, D. De Salvador, E. Napolitani, A. V. Drigo, and A. Carnera, *Appl. Phys. Lett.* **83**, 680 (2003).

<sup>6</sup>G. Mannino, N. E. B. Cowern, F. Roozeboom, and J. G. M. van Berkum, *Appl. Phys. Lett.* **76**, 855 (2000).

<sup>7</sup>D. De Salvador, E. Napolitani, G. Bisognin, A. Carnera, E. Bruno, S. Mirabella, G. Impellizzeri, and F. Priolo, *Appl. Phys. Lett.* **87**, 221902 (2005).

<sup>8</sup>P. A. Stolk, H.-J. Gossmann, D. J. Eaglesham, D. C. Jacobson, J. M. Poate, and H. S. Luftman, *Appl. Phys. Lett.* **66**, 568 (1995).

<sup>9</sup>F. Cristiano, X. Hebras, N. Cherkashin, A. Claverie, W. Lerch, and S. Paul, *Appl. Phys. Lett.* **83**, 5407 (2003).

<sup>10</sup>N. Cherkashin, M. Hytch, F. Cristiano, and A. Claverie, *Solid State Phenom.* **108/109**, 303 (2005).

<sup>11</sup>S. Mirabella, A. Coati, D. De Salvador, E. Napolitani, A. Mattoni, G. Bisognin, M. Berti, A. Carnera, A. V. Drigo, S. Scalese, S. Pulvirenti, A. Terrasi, and F. Priolo, *Phys. Rev. B* **65**, 045209 (2002).

<sup>12</sup>W. Luo, P. B. Rasband, P. Clancy, and B. W. Roberts, *J. Appl. Phys.* **84**, 2476 (1998).

<sup>13</sup>M. Cogoni, A. Mattoni, B. P. Uberuaga, A. F. Voter, and L. Colombo, *Appl. Phys. Lett.* **87**, 191912 (2005).

<sup>14</sup>G. Bisognin, D. De Salvador, E. Napolitani, A. Carnera, E. Bruno, S. Mirabella, F. Priolo, and A. Mattoni, *Semicond. Sci. Technol.* **21**, L41 (2006).

<sup>15</sup>J. S. Christensen, H. H. Radamson, A. Y. Kuznetsov, and B. G. Svensson, *Appl. Phys. Lett.* **82**, 2254 (2003).